Stabilization of stationary excitation pulses in an open flow without long-range inhibition

Mads Kærn
Center for BioDynamics and Department of Biomedical Engineering, Boston University, 44 Cummington Street, Boston, Massachusetts 02215

Michael Menzinger
Department of Chemistry, University of Toronto, 80 St. George Street, Toronto, Ontario, Canada M5S 3H6
(Received 5 September 2001; published 15 March 2002)

We study numerically and experimentally the stabilization of stationary excitation pulses in an open flow system. Since all the species have equal flow and diffusion coefficients, stabilization of stationary pulses by long-range inhibition is excluded. Upstream propagating pulses slow down as they approach the inflow boundary, where a constant forcing establishes a downstream extending subexcitable boundary layer. When the flow velocity is low, successive pulses vanish as they reach the subexcitable region. When the flow velocity is increased, the incoming pulses pile up near the inflow one after the other to form a stationary and space-periodic structure. This occurs in such a manner that the system remembers and stores the number of incoming pulses. We show that flow-induced stabilization of stationary pulses involves a mechanism by which the upstream subexcitable region and the flow cause the arrest of the pulse front and the pulse back, respectively. We discuss how the flow-stabilized structures compare to, and are different from those stabilized by a long-ranged, diffusive inhibition and from those observed in boundary-forced open flows of media showing relaxation-type oscillations.

DOI: 10.1103/PhysRevE.65.046202 PACS number(s): 05.45.−a, 47.70.−n, 82.20.−w

I. INTRODUCTION

The formation of sustainable stationary structures in dissipative systems has for many years been a central area of nonlinear science and pattern formation. In reaction-diffusion systems of the activator-inhibitor type, one usually distinguishes between two classes of structures. The first class includes the classical Turing structures [1–3], where the symmetry breaking occurs as the result of fast inhibitor diffusion that destabilizes the homogeneous steady state. In the second class of structures, the homogeneous steady state remains stable to small amplitude fluctuations and symmetry breaking requires a finite and localized perturbation to be applied. These structures are typically associated with bistable and excitable local kinetics [4–10] and they also require a rapidly diffusing inhibitor, i.e., a long-range inhibition.

In recent years, there has been an increasing interest in the spatiotemporal dynamics of boundary-forced open flows. While it has been known for some time [11,12] that the behavior of convectively unstable open flows is determined by the dynamics at the inflow boundary, the implications of this ability to exert a *global organization* due to a *local forcing* have yet to be fully explored. For instance, it was only recently predicted theoretically [13,14] and verified experimentally [15] that the constant boundary forcing of open flows of oscillatory media may cause the formation of stationary space-periodic structures without a rapidly diffusing inhibitor. These essentially kinematic ''flow-distributed oscillations'' (FDO) are the result of a boundary forcing that locks the oscillation phase at the inflow while the flow resolves the oscillation spatially. As a result, FDO waves are in general confined to the region of parameter space where the local kinetics is oscillatory [14–16]. Exceptions to this rule are found in systems with subcritical behavior [17] and systems with differential transport [18], where space-periodic structures were found to exist outside the region of oscillatory local kinetics.

In this paper, we investigate numerically and experimentally the effect of constant boundary forcing on an open flow of an excitable medium where all flow and diffusion coefficients are equal. A number of recent studies of pulse propagation in flow systems have focused on the effect of nonuniform flow profiles [19–22], differential flows [23], and on the effect of hydrodynamics (see, e.g., Refs. [24–27]). To the best of our knowledge, global organization due to forcing at the inflow boundary has not previously been considered in excitable open flows. The present study is further motivated by our earlier work on boundary-forced open flows of oscillatory media showing oscillations of the relaxation type [15,28,29]. Although the FDO mechanism cannot be responsible for the formation of stationary structures in the excitable regime, it is known from studies of reaction-diffusion systems that excitable media may show structures, such as target patterns and spirals, that are superficially similar to structures observed in oscillatory media of the relaxation type [30]. On this basis, we hypothesized that excitable open flows may be able to support stationary structure that in some aspects are similar to FDO waves but are governed by an entirely different mechanism.

In Sec. II, we show that stationary, space-periodic structures are indeed supported in the boundary-forced open flow of an excitable medium. Stationary space-periodic structures arise when excitation pulses, emitted periodically from a downstream pacemaker, propagate upstream against the flow, slow down and come to a rest near a constantly forced sub-

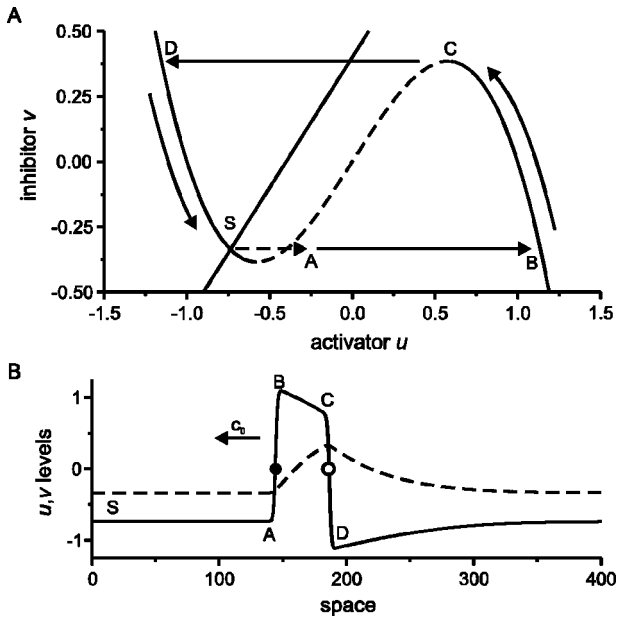

FIG. 1. (a) Phase plane of an excitable medium. The two nullclines intersect at a unique steady-state *S*. A finite perturbation may bring the system across the unstable branch of the activator nullcline (broken line) to point *A*. Activator accumulates rapidly to point *B* and the system returns to *S* following a trajectory through points *C* and *D*. (b) Excitation pulse in an excitable reaction-diffusion system. The pulse profile, full line for the activator, broken line for the inhibitor, is dictated by the local kinetics and the nullcline structure, as described in the text. The front and back of the pulse is indicated by closed and open circle, respectively. The reaction-diffusion velocity is denoted by c_0. The pulse moves to the left.

excitable inflow boundary. In contrast to FDO waves, a specific boundary forcing is required and a domain-filling structure is not formed spontaneously. Instead, a space-periodic structure is established by the piling up of incoming pulses such that the system remembers and stores the number of large amplitude perturbations applied downstream. Hence, the stationary structures observed in the excitable region are the result of a mechanism that is unrelated to the FDO mechanism. In fact, the observed structures turn out to be closely related, at least mechanistically, to the stationary structures stabilized by long-range inhibition. However, despite the mechanistic difference, the domain-filling structures formed in the excitable region by applying multiple perturbations are indistinguishable from and superficially identical to waves observed in the region showing relaxation oscillations.

The numerical predictions are verified experimentally using the Belousov-Zhabotinsky (BZ) reaction medium. Both the simulations and the experiments show that the flow velocity has to exceed a certain critical value for the stationary structures to form. From studies of reaction-diffusion systems, it is well known that an excitation pulse is annihilated when it enters a subexcitable region where the excitation threshold (e.g., the level of inhibitor) is too high to support further propagation of the pulse. Hence, an increased flow velocity exerts somehow a stabilizing effect on stationary excitation pulses, which are unstable in the absence of a flow or at low-flow velocities. Before the experimental verification in Sec. IV, we discuss in Sec. III the qualitative basis of this flow-induced stabilization. It is shown that the formation of a stable stationary pulse is the result of a mechanism by which an upstream subexcitable region, established by the boundary forcing or by a previously stabilized stationary pulse, arrests the pulse front, while the flow causes the front back to come to a rest downstream of the motionless pulse front.

II. NUMERICAL SECTION

A prototype model of an excitable flow system is the FitzHugh-Nagumo (FHN) reaction-diffusion system augmented with flow terms. The FHN system is a generic model of excitable systems and diffusion-induced stabilization of stationary excitation pulses due to long-range inhibition is well understood in this system [4–10]. The experiments presented in Sec. IV involve the ferroin-catalyzed BZ reaction. This reaction can be modeled fairly well using Oregonator type models. However, there is for the present purpose no qualitative difference in the excitable properties of the two types of models and we have for generality chosen the simpler FHN system.

It is assumed that the activator u and the inhibitor v flow at the same velocity, ϕ. The FHN-flow-diffusion system is given by

$$\frac{\partial u}{\partial t} = u - u^3 - v - \phi \frac{\partial u}{\partial x} + D_u \frac{\partial^2 u}{\partial x^2},$$
$$\frac{\partial v}{\partial t} = \epsilon(\alpha u - v + \beta) - \phi \frac{\partial v}{\partial x} + D_v \frac{\partial^2 v}{\partial x^2}, \tag{1}$$

where α, β, and $\epsilon \ll 1$ are kinetic constants and ϕ is the flow velocity. D_u and D_v are the diffusion coefficients of u and v, respectively. They are assumed to be equal, $D = D_u = D_v$.

The simulations presented below involve a constantly forced inflow boundary at $x = 0$ and a no-flux boundary at $x = L$. It is however useful first to consider the behavior of Eq. (1) in an infinite domain. It is easy to show that in a domain of infinite extent, the flow term in Eq. (1) can be eliminated by changing to the reference frame, $z = x - \phi t$, that moves with the flow. Hence, sufficiently far from the inflow boundary, Eq. (1) behaves as a reaction-diffusion system that is translated through space.

The local dynamics of the excitable FHN system is summarized in Fig. 1(a). The system can be either monostable, bistable, or oscillatory. The system is confined to the *N*-shaped activator nullcline, $v = u - u^3$, when the time-scale separation is large, $\epsilon \ll 1$. The relaxation oscillation, which arises when the steady-state *S* is located between the extremes of the activator nullcline, involves fast transitions between the stable branches of the activator nullcline. The steady state is unique and excitable when the nullclines intersect once on one of the stable branches of activator nullcline. Bistability occurs when the inhibitor nullcline,

$v=\alpha u+\beta$, intersects both of the the stable branches of the activator nullcline, e.g., when its slope α is relatively low. Note that α is the rate constant for the accumulation of inhibitor in the high-activator state where $u>0$ and of inhibitor depletion in the low-activator state where $u<0$. If the FHN kinetics supports a unique and excitable steady state $S=(u_s,v_s)$, as illustrated in Fig. 1(a), a change from excitability to bistability ensues when α is decreased. As it will be discussed in Sec. III, decreasing the rate of inhibitor accumulation within the excited, high-activator state is central to the formation of stationary excitation pulses.

When the system rests in the excitable steady state [marked *S* in Fig. 1(a)], a perturbation that takes the system across the unstable branch of the activator nullcline causes a large excursion in phase space. The initial autocatalytic excitation and the subsequent recovery follows a trajectory through the points *A*, *B*, *C*, and *D* indicated in Fig. 1(a). The initial perturbation, indicated by a broken arrow, takes the system to point *A*. From *A*, there is a very rapid autocatalytic growth of the activator, which brings the system to point *B* on the activator nullcline. The inhibitor accumulates in this region of phase space and the system slowly moves along the activator nullcline toward the saddle point at *C*. Once the system passes through the saddle point, the activator is rapidly depleted and the system is taken to point *D* on the left branch of the activator nullcline. The inhibitor is depleted in this refractory phase and the system slowly returns to the steady-state *S*.

The behavior of excitation pulses in a reaction-diffusion system is closely tied to the local nullcline structure. Figure 1(b) shows the activator and inhibitor profiles for a propagating excitation pulse in the absence of a flow or in the moving reference frame $z=x-\phi t$. The letters on the pulse profile mark the corresponding points A–D in phase space [Fig. 1(a)]. The propagation of the pulse is driven by the autocatalytic growth of the activator and the velocity of the pulse is determined by the velocity c_0 of this autocatalytic front (marked with a closed circle). The reaction-diffusion velocity c_0 depends on the magnitude of the diffusion coefficient *D*, the rate constant of the autocatalytic reaction [unity in Eq. (1)], and on the level of the inhibitor $v(x)$ ahead of the autocatalytic front. In Fig. 1(b), the region ahead of the front is in the stable steady state with $v(x)=v_s$. The propagation velocity increases (lower excitability threshold) if $v(x)<v_s$, while it decreases if the inhibitor level ahead of the front is higher than the steady-state level, $v(x)>v_s$. When $v(x)$ exceeds a certain critical value, the excitability threshold is too high to support propagation. A region where a high level of $v(x)$ prevents the propagation of the autocatalytic front is referred to as *subexcitable* [31]. An example of a subexcitable region is the early part refractory phase that follows after the rapid depletion of the activator, i.e., near the point marked *D* is Fig. 1(b).

When the pulse is sufficiently far from the constantly forced inlet, the effect of the flow is to translate the propagating pulse in the downstream direction. The pulse velocity is thus given by $c=\phi-c_0(v_s)$, where v_s denotes the steady-state level of the inhibitor. Upstream propagation is only supported if the flow velocity is below a critical value, ϕ_c where

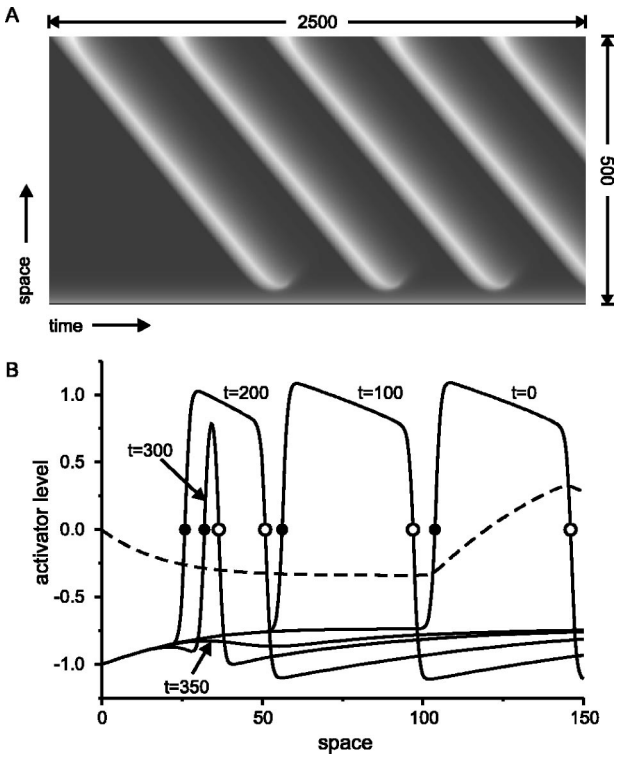

FIG. 2. Excitation pulses vanish when they interact with a subexcitable inflow boundary at low flow velocity, $\phi=0.3$. (a) Space-time plot showing the fate of pulses initiated periodically at the outflow boundary. White corresponds to a high level of activator. The length of the system is 500 space units. The system was integrated for 2500 time units. (b) The activator profile (full lines) at different times. The broken line shows the inhibitor profile at $t=0$. The pulse collapses as the front and the back of the pulse collide. Other parameter values are $\alpha=1$, $\beta=0.4$, $\epsilon=0.01$, and $D=1$.

the tendency of the autocatalytic front to spread upstream is exactly counterbalanced by the flow $[\phi_c=c_0(v_s)]$. The pulse can hence be made stationary by setting the flow velocity equal to ϕ_c. The critical flow velocity corresponds, at least in a bistable system, to the transition between nonlinearly convective ($\phi>\phi_c$) and nonlinearly absolute ($\phi<\phi_c$) unstable flow conditions [32]. Any perturbation is eventually washed out of the system when $\phi>\phi_c$ and interaction with the inflow boundary will occur only in the nonlinearly absolute unstable regime, i.e., when $\phi<\phi_c$.

Figure 2(a) illustrates what may happen when successive upstream propagating pulses interact with a constantly forced inflow boundary at a relatively low-flow velocity of $\phi=0.3$. Multiple pulses are initiated by applying at regular time intervals an excitatory perturbation at the downstream boundary, located at $x=L$ with $L=500$. The state at the inflow boundary is chosen to be $u(x=0)=-1$ and $v(x=0)=0$. The relatively high level of inhibitor at the boundary establishes a downstream extending subexcitable boundary layer [see Fig. 2(b)]. As a consequence, the upstream propagating pulses vanish before they can reach the inflow boundary.

Figure 2(b) shows in more detail the fate of a pulse as it propagates deeper into the inhibitor-rich region near the inflow. It shows in full lines the activator profile at different

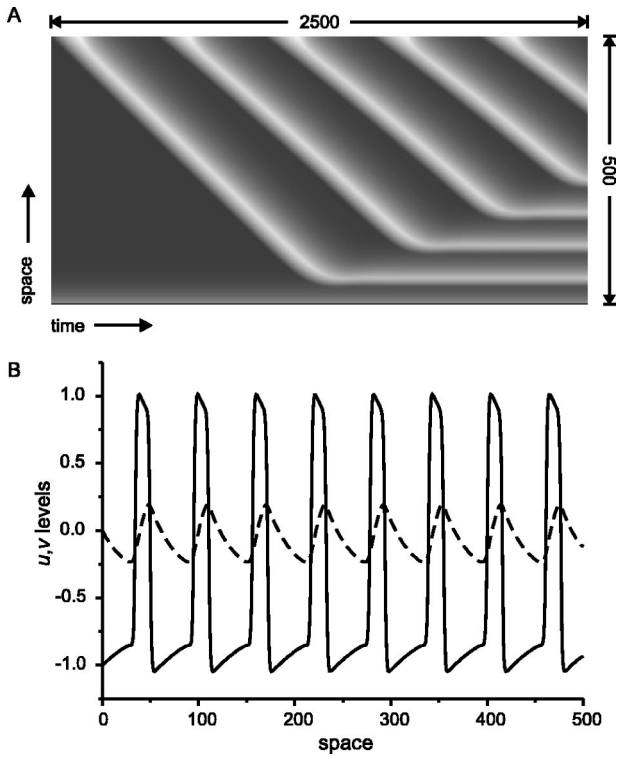

FIG. 3. Formation of a space-periodic structure in a simulation identical to the one in Fig. 2 except for $\phi=0.4$. (a) Pulses are initiated periodically at the outflow boundary. Rather than disappearing as in Fig. 2, subsequent pulses become stationary and stack up one after the other to form a space-periodic structure. (b) The activator and inhibitor profiles for a stationary structure comprised of eight stationary flow-stabilized pulses.

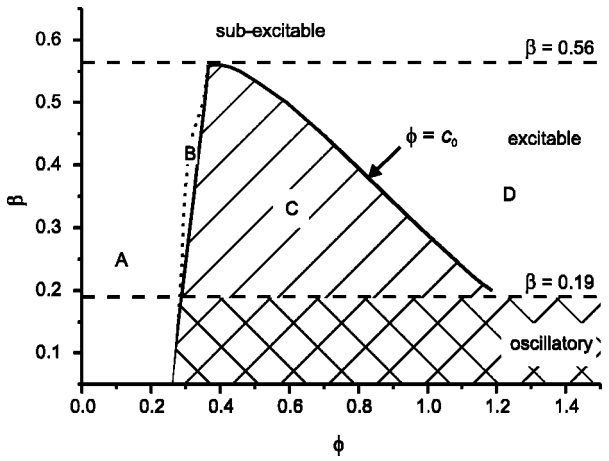

FIG. 4. Region of different spatiotemporal behavior for $\alpha=1$, $\epsilon=0.01$, and $D=1$. The regions marked *A*, *B*, and *C* are associated with vanishing pulses, pulsating structures, and stationary pulses, respectively. Upstream propagation is not supported in the region marked *D*. The system is subexcitable when $\beta>0.56$ and shows relaxation oscillations when $\beta<0.19$. Space-periodic structures are formed spontaneously in the latter region.

times. The broken line shows the inhibitor profile at $t=0$. It is included to illustrate the increasing inhibitor level near the inlet. The autocatalytic pulse front is marked by a closed circle and the pulse back is marked by an open circle. The pulse is observed to slow down as it approaches the inflow. This is due to the gradual increase in inhibitor levels ahead of its autocatalytic front. Eventually, the velocity, $c[v(x)]=c_0[v(x)]-\phi$, of the autocatalytic front reaches zero and the front is at rest at $t=200$. However, the arrest of the autocatalytic front does not mean that the pulse becomes stationary. As it is dictated by the local kinetics (Fig. 1), inhibitor continues to accumulate within the pulse and the back of the pulse (open circle) continues to propagate. The result is a steady decrease in the width of the pulse. At $t=300$, the pulse is very narrow and it has vanished at $t=350$. Note how the autocatalytic front is pushed slightly downstream before the front and the back collides. The reason for this is addressed in Sec. III.

Figure 3(a) shows the dramatic effect of increasing the flow velocity to $\phi=0.4$ in a simulation that is otherwise identical to the one shown in Fig. 2(a). The successive pulses now stack up, one after the other, to form a space-periodic stationary structure that, if a sufficient number of perturbations are applied, eventually fills the entire domain [Fig. 3(b)]. Increasing the flow velocity from 0.3 to 0.4 thus causes the stabilization of a structure that is unstable at low-flow velocity (Fig. 2) or in the absence of a flow.

The space-periodic structure shown in Fig. 3(b) is composed of eight spatially repeating units, each one being a flow-stabilized stationary pulse. The conditions for the stabilization of the first and the second pulse are generally not the same since the formation of the first pulse is sensitive to the state imposed at the inflow boundary. It is possible to find boundary conditions where the first pulse becomes stationary while any subsequent pulse that enters its subexcitable refractory tail vanishes (not shown). In the present case, however, the state at the boundary was chosen to correspond to an early stage of the refractory phase. The conditions for the stabilization of any subsequent pulses are therefore the same as for the first one and there is a one-to-one correspondence between the number of units in the structure and the number of perturbation applied at the downstream boundary. Applying one perturbation gives a stable structure composed of one flow-stabilized stationary pulse; applying two perturbations gives a stable structure comprised of two pulses, etc. In other words, when the distance between two flow-stabilized stationary pulses is λ, a system of length L is multidegenerate with a total of $n=L/\lambda$ different nonuniform stationary states.

Figure 4 summarizes the regions of the β, ϕ parameter space where different pulse behavior was observed in numerical simulations. The system is subexcitable when β is greater than about 0.56 and it does not support upstream propagating pulses at any flow velocity. In the region marked "*A*," pulses collapse when they reach the subexcitable region near the inflow boundary. Stationary structures are observed in the region marked "*C*." For $\beta>0.19$, space-periodic structures are only formed if multiple excitations are applied. In the region of parameter space where the FHN system shows relaxation oscillations ($\beta<0.19$), the domain-filling space-periodic structure is formed spontaneously and external perturbations are not necessary. In the region marked "*B*," the first pulse persists, but does not become

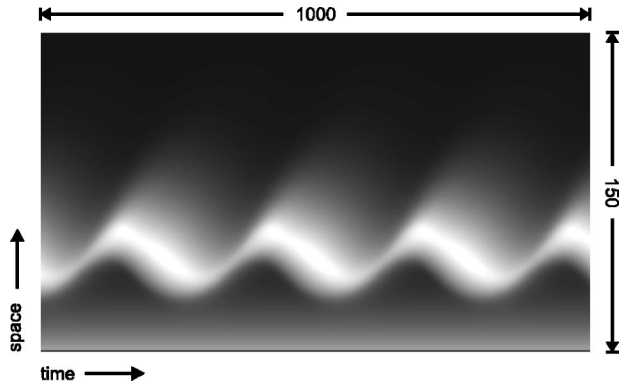

FIG. 5. Example of a solitary pulsating structure established at the edge of the subexcitable region. Parameter values are the same as in Fig. 2 except for ϕ which is increased to $\phi=0.31$. The figure shows 1000 time units and 150 space units. The oscillation period is about 290 time units long.

stationary. Instead, it performs an oscillatory motion at the edge of the subexcitable region as shown in Fig. 5. This behavior is discussed in more detail in Sec. III. The relaxation time may be quite long near the *BC* boundary as each subsequent pulse may settle at a fixed location through a long-lived damped oscillation. No upstream propagating pulses are observed in the region labeled "*D*" where the flow velocity exceeds the reaction-diffusion velocity, $c_0(v_s)$, of the pulse.

In the oscillatory region, the spontaneous formation of domain-filling space-periodic patterns can be understood in terms of the FDO mechanism. Multiple perturbations are not required in order to create a domain-filling structure and the degeneracy of available stationary states is lost. The domain-filling structures formed in the oscillatory and in the excitable regions of parameter space are however indistinguishable from each other. This is demonstrated in Fig. 6 where the wavelength is plotted as a function of β. The transition from excitable to oscillatory local dynamics is accompanied by a destabilization of the homogeneous state through a Hopf bifurcation. There is however no quantitative or qualitative change in the domain-filling structure at the critical point β_{Hopf} where a limit cycle solution is born.

III. FLOW-INDUCED STABILIZATION

In order to gain further insights into the mechanism of flow-induced stabilization, we consider the results in Figs. 2 and 3. Figure 7, shows how the activator profile changes as a pulse slows down and becomes stationary by interacting with the constantly forced inflow. All parameter values are the same as in Fig. 3, but only the first pulse is considered. As in Fig. 2, the velocity of the autocatalytic front, marked by a closed circle, decreases to zero as it reaches the subexcitable region. In contrast to the low-flow simulation in Fig. 2, the back of the pulse comes in Fig. 7 to a rest at a finite distance from the arrested autocatalytic front. Thus, the formation of a stationary pulse is the result of the front (closed circle) and the back (open circle) of the pulse never colliding and an elevated flow velocity somehow prevents the propagation of the back of the pulse(s).

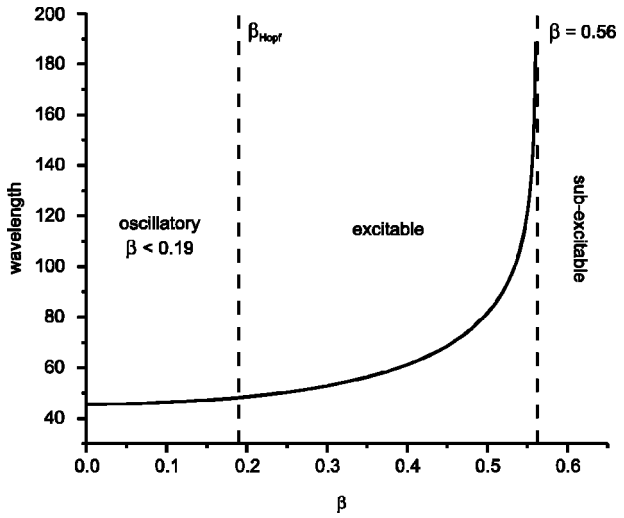

FIG. 6. The wavelength is continuous at the transition from excitable to oscillatory local dynamics. The space-filling structure formed by the FDO mechanism is indistinguishable from that composed of multiple stationary flow-stabilized pulses. Parameter values are $\alpha=1$, $\epsilon=0.01$, $D=1$, and $\phi=0.3$.

The ability of a flow to arrest back of a pulse stems from the marginal differences in phase plane structure of excitable and bistable media and from the fact that an excitable system can be converted into a bistable system by a slight shift in the inhibitor nullcline (see Sec. II). This slight shift however has profound implications for the local dynamics since the presence of a steady state on the right branch of the activator nullcline prevents the inhibitor from accumulating to the saddle point (point *C* in Fig. 1) where the activator is rapidly depleted. In other words, a small shift in the phase plane structure is sufficient to maintain the system in an excited, high activator state indefinitely.

As discussed in Sec. II, a transition from excitability to bistability occurs in the FHN system when the value of the α is decreased, i.e., when the rate of the inhibitor accumulation in the high-activator state is lowered. An increased flow has

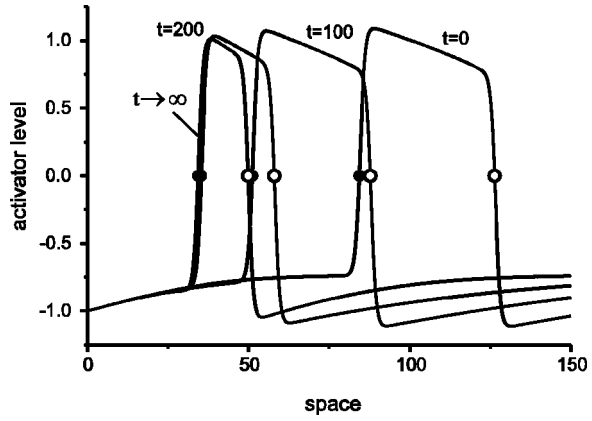

FIG. 7. Activator profiles at different times during the flow-induced stabilization of the first pulse in Fig. 3. The back of the pulse slows down and comes to a rest at a distance from the autocatalytic front and the pulse can thus maintain a finite width indefinitely.

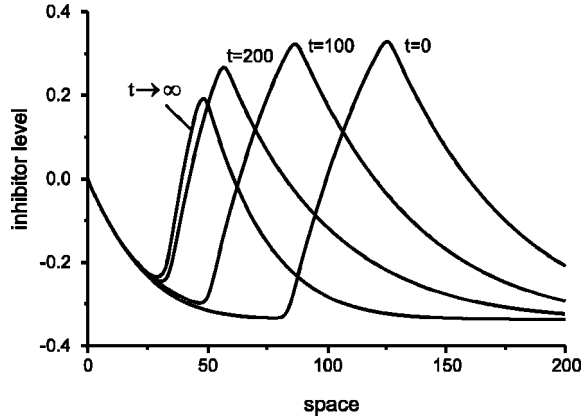

FIG. 8. Inhibitor profiles at different times during the formation of the first stationary pulse in Fig. 3. The profile becomes steeper within the pulse at the front as the width of the pulse decreases.

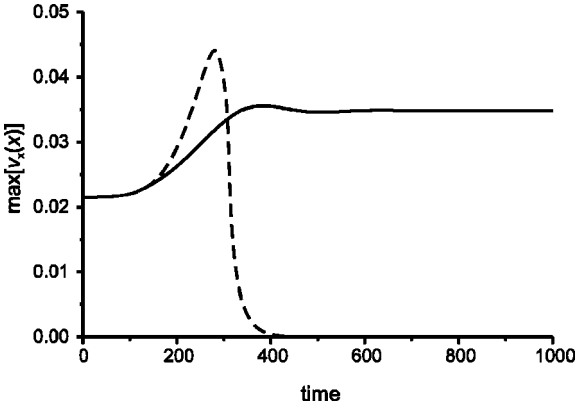

FIG. 9. The evolution of the maximal value of $v_x(x)$ during the formation of the first stationary pulse in Fig. 3 (full line) and during the collapse of the first pulse in Fig. 2 (broken line).

a similar effect. As dictated by the local kinetics, the inhibitor gradient, $v_x(x)=\partial v/\partial x$, is positive in the portion of the pulse where activator levels are high. This is clearly seen in Fig. 1(b). The flow term, $-\phi v_x(x)$ in Eq. (1), is therefore negative within the pulse. As a result, the flow causes the local rate of inhibitor accumulation to decrease.

We know that the flow term counterbalances the rate of inhibitor accumulation at the critical flow velocity ϕ_c where the entire pulse is stationary. The same can be achieved at sub-critical flow velocities provided that the autocatalytic front slows down and comes to a rest. Figure 8 shows how the inhibitor profile changes as a pulse slows down and becomes stationary. The parameter values are the same as those in Fig. 3. Once the autocatalytic front is at rest, the continued propagation of the pulse back causes the region of high activator to narrow (see Fig. 7). This, in turn, causes the inhibitor profile to become steeper and the flow term, $-\phi v_x(x)$, to become more negative. Eventually, the flow term becomes sufficiently negative to prevent further accumulation of the inhibitor. As a result, inhibitor never reaches the level of the saddle point (point *C* in Fig. 1), rapid depletion of activator is prevented and the pulse back comes to rest. The flow thus plays the same role as does fast inhibitor diffusion during the stabilization of stationary excitation pulses in reaction diffusion. In both cases, rapid removal of inhibitor from within the activator-rich region of the pulse prevents the inhibitor from accumulating to the level where activator is rapidly depleted. Since a decreased rate of inhibitor accumulation causes the excitable system to become bistable, we may say that the effect of a flow and of rapid inhibitor diffusion is to cause a local bistability within the activator-rich portion of the pulse.

The steepness of the inhibitor profile depends on the distance between the pulse front and the pulse back. It continues to increase as the pulse narrows. It thus seems paradoxical that stationary pulses cannot form at low-flow velocity. The flow should be able to prevent the local accumulation of inhibitor when $\max[v_x(x)]$ has increased to an appropriate value. This argument, however, ignores the fact that an increased steepness of the inhibitor profile also causes an increase in the upstream diffusive flux of the inhibitor. The temporal evolution of the maximal value of $v_x(x)$ is shown in Fig. 9. The full line shows the evolution of $\max[v_x(x)]$ to a constant level as the first pulse in Fig. 3(a) slows down and becomes stationary. The broken line shows the evolution of $\max[v_x(x)]$ for a pulse that collapses at low-flow velocity. As expected, the value of $\max[v_x(x)]$ becomes higher at the low-flow velocity, but a stationary pulse nevertheless fails to establish. The reason for this is fairly simple. Recall, that the autocatalytic front comes to rest within the region of reduced excitability where the flow counterbalances its reaction-diffusion velocity. The front initially comes to rest exactly at the edge of the subexcitable region established by the boundary forcing where $\phi=c_0[v(x)]$. However, the gradual increase in the inhibitor gradient within the pulse causes the inhibitor levels ahead of the autocatalytic front to increase. As a result, the region where the autocatalytic front is at rest becomes subexcitable. Now the flow velocity exceeds the reaction-diffusion velocity, $\phi>c_0[v(x)]$, and the autocatalytic front is pushed downstream into the oncoming pulse back [see Fig. 2(b)]. This causes the pulse to vanish at low flow velocity.

If the flow velocity is the right range, however, the front and back of the pulse may not collide as the front is pushed downstream. The inhibitor level ahead of the pulse may have sufficient time to return to its original value before the collision occurs. As the region ahead of the front regains excitability, a front that was initially pushed downstream may again move upstream. Once it has come to rest, there is a buildup of a steep inhibitor profile within the pulse and the process repeats itself. This alternating upstream and downstream motion of the front gives rise to a *pulsating structure*, i.e., a pulse that periodically moves up- and downstream, as it was shown in Fig. 5.

IV. EXPERIMENTAL SECTION

The experimental verification of flow-induced stabilization was carried out using the excitable BZ reaction medium. A mixture containing $[H_2SO_4]=0.16\,M$, $[BrO_3^-]=0.10M$, $[\text{ferroin}+\text{ferriin}]=4.0\times10^{-3}M$ and $[\text{malonic acid}]=0.020M$, was pumped through a packed bed

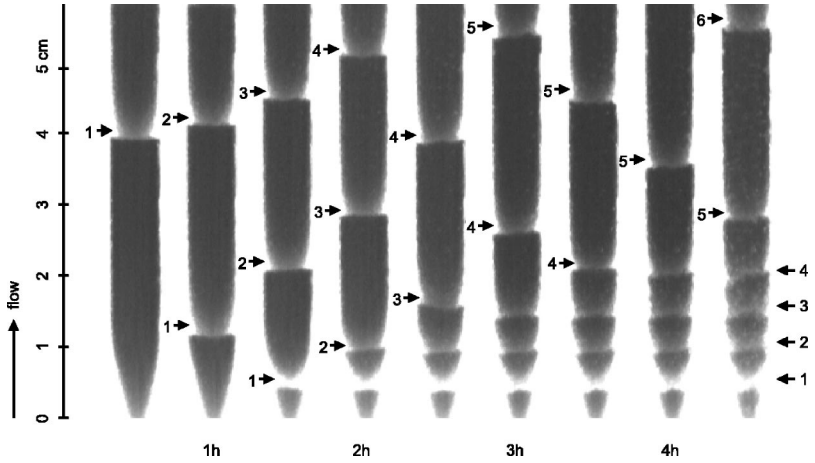

FIG. 10. Experimental observation of flow-induced stabilization at $\phi = 0.12$ cm/min. White bands correspond to regions of high ferriin concentration. The snap shots of the flow reactor are taken at intervals of 30 min. The labeled arrows indicate the location of subsequent pulses. Note that the first few pulses become stationary in the region where the flow velocity is increased due to the conical shape of the reactor inlet.

reactor (PBR) using a peristaltic pump. The PBR was a 20-cm-long 0.635-cm inner-diameter glass tube filled with 500 μm glass beads to various heights. It had a conical-shaped inlet. The liquid medium was removed by suction such that the outflow boundary of the PBR coincides with the height of the glass beads.

The vertically mounted PBR was illuminated from the back by two fluorescent tubes. The propagation of excitation pulses was monitored using a charged-coupled device camera fitted with a 450–550 nm bandpass filter. This setup allows for the detection of bands of oxidized blue ferriin complex, a precursor for the inhibitor, bromide, as white on a black background.

The glass beads ensures that the flow field is more or less uniform (''plug flow''). The one-dimensional description in Eq. (1) is a fairly good approximation even at low-flow velocities. While incomplete mixing within the packed bed and an inhomogenous flow field does affect the propagation of excitation pulses [33], there were no indications that such factors significantly alter the formation of flow-stabilized structures.

Preliminary experiments showed that spontaneous excitation occurs for all bromate concentrations between 0.03 and 0.14 M. It manifests itself simultaneously over a long length scale and appears to be the result of a very slow oscillation. The period of oscillation was estimated to be about 80 and 30 min for bromate concentrations of 0.03*M* and 0.14*M*, respectively. Spontaneous excitation is suppressed only if the solution is open to air in a stirred batch reactor. The oscillation appears to be the result of a slow bromide-generating step that is inhibited in the presence of molecular oxygen [R. Fields private communication]. The time before the first oscillation-induced excitation is about 46 min when $[BrO_3^-] = 0.10M$. During this time period, as many as nine excitation pulses were emitted when a 1-mm-thick silver wire was inserted between glass beads at the upper end of the reactor (not shown). The first six pulses were emitted at intervals of ~ 4.4 min. The result of this tenfold difference in time-scales is that the slow oscillation does not manifest itself and does not interfere with the excitation pulses, at least when the residence time in the flow reactor, defined as $\tau = L/\phi$, is kept less than or comparable to the oscillation period.

The BZ reaction medium originated from a continuously stirred tank reactor (CSTR). Special care was taken to ensure that the state of the medium in the CSTR corresponds to a point early in refractory phase. The subexcitable state of the CSTR establishes a boundary layer near the PBR inlet where the medium has reduced excitability. The experimental setup used to achieve this is described in detail elsewhere [33].

Figure 10 displays nine snapshots showing about 5.8 cm of the PBR and taken at half hour intervals. The flow velocity is 0.12 cm/min and the flow is directed upward, against gravity. Volume elements spend about $\tau = 48$ min in the displayed region and the residence time of the roughly 7-cm-long PBR is about 60 min. Since the residence time τ is longer than the oscillation period $T = 46$ min, it is expected that a spontanous excitation, due to the presence of the slow oscillation should occur 46 min into experiment at a distance of about $\phi T = 5.5$ cm from the inlet. However, a large number of excitation pulses can be generated during this time period and diffusion-induced excitation occurs before the oscillation-induced excitation in a reactor of this length at this flow velocity. As a result, the system behaves in all aspects as if the medium was excitable and the slow oscillation does not manifest itself in Fig. 10.

Subsequent excitation pulses are initiated at the outflow by inserting a silver wire into the glass beads. The wire was kept in the PBR for the first hour of the experiment. A single pulse (labeled 1) is visible 30 min after the experiment was started. At this time it is located about 4 cm from the inflow. Thirty minutes later it has moved about 2.8 cm upstream at an average velocity of 0.09 cm/min. During the two subsequent 30 min intervals it first travels 0.73 and then 0.02 cm. Two hours after the experiment was started, the pulse has come to rest about 0.45 cm from the bottom of the displayed region.

Sixty minutes after the experiment was started, a second pulse, labeled 2 in Fig. 10, is visible at a distance of about 3.9 cm from the boundary. It propagates at a velocity that is significantly decreased compared to that of the preceding pulse in the same region of the reactor. This is presumably due to an increased excitability threshold of the medium, induced by the passage of the first pulse. After about 2.5 h it comes to rest little more than 0.5 cm behind the first pulse. The same behavior is observed for each subsequent pulse

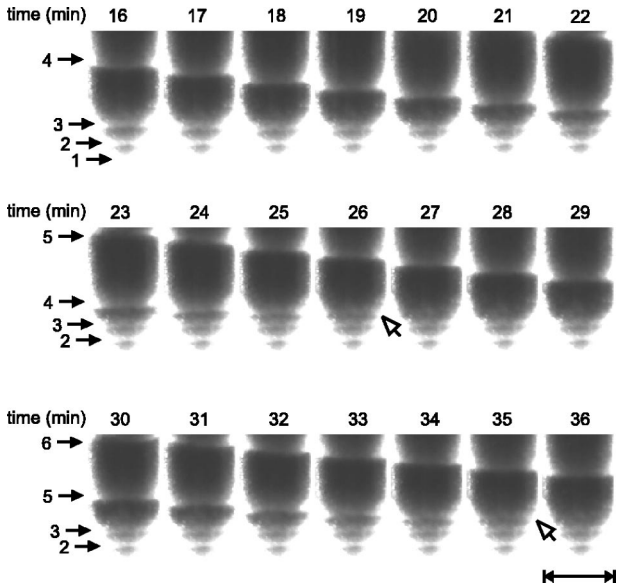

FIG. 11. Flow-induced stabilization requires a super-critical flow velocity. Snapshots of the flow reactor taken one minute apart are shown next to each other with time proceeding from left to right. Each row corresponds to 7 min. The bar corresponds to 1 cm. The first displayed snapshot was taken 16 min after the experiment was started. At this time, three pulses (labeled 1–3) are observed in the region where the flow velocity is high due to the conical shape of the reactor and one pulse, labeled 4, is located at a distance of about 2 cm from the reactor inlet. This pulse propagates upstream with a decreasing velocity. It has vanished at $t=27$ min. The same behavior is observed for the pulse labeled 5, which has vanished at time $t=35$ min. The pulses vanish at a distance from the reactor inlet where the flow velocity is about 0.07 cm/min (indicated by arrow).

(labeled 3, 4, and 5), which stack up, one after the other to form a fairly space-periodic structure with a wavelength of about 0.52 cm.

Once the space-periodic structure has been established, a volume element that is carried downstream from the inlet experiences an excitation at regular intervals. When assuming a constant flow velocity of 0.12 cm/min, i.e., neglecting the conical narrowing of the PBR, a volume element carried through the space-periodic structure experiences an excitation roughly every $T=0.52/0.12$ min$=4.3$ min. In the absence of a flow, the time interval between the emission of pulses is determined primarily by the time it takes for the system to recover excitability during the refractory phase. The good agreement between the time interval of excitation observed in the presence (~ 4.3 min) and in the absence of a flow (~ 4.4 min) suggests that the wavelength of the space-periodic structure also depends on the time it takes to recover excitability.

Figure 11 displays snapshots of the region near the reactor inlet in an experiment where the flow velocity is relatively low at about 0.04 cm/min. The length of the PBR is decreased to a length of about 2 cm to prevent spontanous excitation induced by the slow oscillation. The snapshots are taken at intervals of 1 min and are placed in sequence from left to right. The sequence starts with a snapshot taken 16 min after the first pulse was initiated. Four pulses are visible at this time. Two (labeled 1 and 2) are motionless within the conical shaped region near the inlet (pulse 1 is located at the very bottom and its upstream edge is not visible) while the other two (labeled 3 and 4) propagate upstream. Pulse 3 approaches the subexcitable tail of pulse 2 and comes to rest about 0.14 mm from it. The reactor is about 0.45 mm wide at the point where pulse 3 becomes stationary. The flow velocity is estimated to be 0.08 cm/min at this point.

As pulse 4 approaches the motionless pulse 3, it slows down and almost comes to rest after 26 min at a location indicated by the arrow. However, it fails to maintain its amplitude and it has vanished one minute later. The same is observed after 35 min when the fifth pulse approaches the third pulse, as well as any subsequent pulse (not shown). The pulses are annihilated at the same point (indicated by the arrow) where the width of the reactor is about 0.52 cm and the flow velocity is approximately 0.06 cm/min. This demonstrates that a stable stationary pulse can only form if the flow velocity is higher than 0.07 ± 0.01 cm/min. Note that the pulses are perpendicular to the flow. This shows that the system can indeed be approximated by a one-dimensional plug-flow model.

V. DISCUSSION

The formation of static structures in excitable reaction-diffusion media has traditionally been associated with rapidly diffusing inhibitor. The diffusion-stabilized structures are the result of rapid removal of inhibitor from within the front, which has a twofold effect. First, fast inhibitor diffusion slows down the accumulation of inhibitor within the front and prevents it from reaching the critical level where activator is rapidly depleted. Second, fast inhibitor diffusion causes the level of inhibitor ahead of the autocatalytic front to increase. This causes an arrest of the autocatalytic front as the medium ahead of the pulse becomes subexcitable.

This paper has presented experimental and numerical evidence for an alternative mechanism that involves a *flow-induced* rather than a diffusion-induced stabilization. From a mechanistic point of view, the flow affects the dynamics in much the same way as does rapid inhibitor diffusion. Both prevent the accumulation of inhibitor within the pulse, which can introduce a local bistability in the system. This allows the high activator state to persist indefinitely. However, the flow can only counterbalance the upstream propagation of the autocatalytic front at a critical flow velocity. In a bistable system, this flow velocity corresponds to the transition between nonlinearly absolute and convective instability [32]. In order for stationary pulses to establish at subcritical flow velocities, i.e., in the nonlinearly absolute unstable regime, a special boundary condition is needed. This special boundary forcing has to establish a subexcitable region at the inflow such that an incoming autocatalytic front comes to a rest. Once the front is at rest, the flow may stabilize the activator-rich portion of the pulse by preventing local accumulation of inhibitor. After the first stationary pulse is established, its refractory tail constitutes an upstream subexcitable region and the appropriate boundary condition is reestablished. As a

result, subsequently approaching pulses also come to rest and pile up to form a space-periodic structure.

There are other significant differences between flow- and diffusion-induced stabilization. For instance, in a system that supports diffusion-stabilized solitary structures, the pulse cannot propagate very far away from the site where the perturbation was initially applied. This is not so in the flow system, where a pulse continues to propagate until it reaches an upstream subexcitable region. This allows multiple perturbations to be applied at the same spot. At sufficiently high-flow velocities, there is a one-to-one correspondence between the number of perturbations applied and the number of flow-stabilized stationary pulses that stack up near the inflow. An open flow of an excitable medium can thus act as a counting and memory device whose capacity depends linearly on its length. When the distance between subsequent pulses is λ, a system of length L supports a total of $n = L/\lambda$ nonhomogeneous stationary states in addition to the homogeneous steady state. Second, an increased rate of inhibitor diffusion actually has a *destabilizing* effect on flow-stabilized pulses. Increased inhibitor diffusion not only decreases the steepness of the inhibitor profile, but also causes an increase in the upstream flux of the inhibitor. Conversely, the flow-induced stabilization is enhanced when the diffusivity of the inhibitor is reduced. The predicted effects of a changed inhibitor diffusivity have been verified by numerical simulations (not shown).

While there are significant differences between the mechanisms of formation of stationary structures reported here and the FDO waves previously reported [13–15], the visual appearance of the domain-filling structure observed in the excitable region [Fig. 3(b)] is identical to that of spontaneously formed FDO waves in the oscillatory regime. The wavelength of the space-periodic structure extends continuously from one kinetic region to the other. This is not surprising since the global structure of the phase plane does not depend on the local structure near the steady state. For instance, the strong dependence of the FDO wavelength on the diffusion coefficients observed in the oscillatory BZ medium [15] can be understood in terms of the same mechanism that causes arrest of the autocatalytic front under excitable conditions: the autocatalytic front continues to propagate upstream and into the refractory tail of the preceding pulse until its intrinsic velocity $c_0[v(x)]$ is matched by the flow velocity.

Finally, the transient dynamics of patterns formed in an oscillatory medium of the relaxation type might be better understood in terms of excitation pulses than the kinematic FDO mechanism. For instance, under certain conditions, it has been observed [34,35] that some of the incoming waves vanish rather than settling into a stationary pattern. This behavior is inconsistent with a temporal oscillation that is distributed spatially by the flow. It is on the other hand consistent with the dynamics of an excitable medium in the region of parameter space where the refractory tail of the upstream located pulse is slow to settle into the stationary profile required for the flow-induced stabilization of an incoming pulse.

ACKNOWLEDGMENT

The Natural Sciences and Engineering Research Council of Canada provided an operating grant.

[1] A. M. Turing, Proc. R. Soc. London, Ser. B **237**, 37 (1952).
[2] V. Castets, E. Dulos, J. Boissonade, and P. DeKepper, Phys. Rev. Lett. **64**, 2953 (1990).
[3] Q. Ouyang and H. L. Swinney, Nature (London) **352**, 612 (1991).
[4] G. B. Ermentrout, S. P. Hastings, and W. C. Troy, SIAM J. Comput. **44**, 1133 (1984).
[5] K. L. Lee, W. D. McCormick, Q. Ouyang, and H. L. Swinney, Science **261**, 192 (1993).
[6] A. Hagberg and E. Meron, Phys. Rev. E **48**, 705 (1993).
[7] B. N. Vasiev, A. V. Panfilov, and R. N. Khramov, Phys. Lett. A **192**, 227 (1994).
[8] M. Bode and H. G. Purwins, Physica D **86**, 53 (1995).
[9] C. B. Muratov and V. V. Osipov, Phys. Rev. E **54**, 4860 (1996).
[10] A. Hagberg, E. Meron, and T. Passot, Phys. Rev. E **61**, 6471 (2000).
[11] R. J. Deissler, J. Stat. Phys. **40**, 371 (1985).
[12] R. J. Deissler, J. Stat. Phys. **54**, 1459 (1989).
[13] S. P. Kuznetsov, E. Mosekilde, G. Dewel, and P. Borckmans, J. Chem. Phys. **106**, 7609 (1997).
[14] P. Andrésen, M. Bache, E. Mosekilde, G. Dewel, and P. Borckmanns, Phys. Rev. E **60**, 297 (1999).
[15] M. Kærn and M. Menzinger, Phys. Rev. E **60**, 3471 (1999).
[16] J. R. Bamforth, J. H. Merkin, S. K. Scott, R. Tóth, and V. Gáspár, Phys. Chem. Chem. Phys. **3**, 1435 (2001).
[17] J. R. Bamforth, S. Kalliadasis, J. H. Merkin, and S. K. Scott, Phys. Chem. Chem. Phys. **2**, 4013 (2000).
[18] R. Satnoianu and M. Menzinger, Phys. Rev. E **62**, 113 (2000).
[19] C. R. Doering and W. Horsthemke, Phys. Lett. A **182**, 227 (1993).
[20] M. A. Allen, J. Brindley, J. H. Merkin, and M. J. Pilling, Phys. Rev. E **54**, 2140 (1996).
[21] V. N. Biktashev, A. V. Holden, M. A. Tsyganov, J. Brindley, and N. A. Hill, Phys. Rev. Lett. **81**, 2815 (1998).
[22] V. N. Biktashev, I. V. Biktasheva, A. V. Holden, M. A. Tsyganov, J. Brindley, and N. A. Hill, Phys. Rev. E **60**, 1897 (1999).
[23] A. B. Rovinsky, A. M. Zhabotinsky, and I. R. Epstein, Phys. Rev. E **58**, 5541 (1998).
[24] M. Diewald, K. Matthiessen, S. C. Muller, and H. R. Brand, Phys. Rev. Lett. **77**, 4466 (1996).
[25] B. Legawiec and A. L. Kawczynski, J. Phys. Chem. **101**, 8063 (1997).
[26] K. A. Cliffe, S. J. Tavener, and H. Wilke, Phys. Fluids **10**, 730 (1998).
[27] V. Perez-Villar, A. P. Munuzuri, and V. Perez-Munuzuri, Phys. Rev. E **61**, 3771 (2000).
[28] M. Kærn and M. Menzinger, Phys. Rev. E **61**, 3334 (2000).
[29] M. Kærn, M. Menzinger, and A. Hunding, Biophys. Chem. **87**, 121 (2000).

[30] A. S. Mikhailov, *Foundations of Synergetics I* (Springer-Verlag, New York, 1990).
[31] S. Kádár, J. Wang, and K. Showalter, Nature (London) **391**, 770 (1998).
[32] J. M. Chomaz, Phys. Rev. Lett. **69**, 1931 (1992).
[33] M. Kærn and M. Menzinger, J. Phys. Chem. A (to be published).
[34] J.R. Bamforth, R. Tóth, V. Gáspár, and S. K. Scott, Phys. Chem. Chem. Phys. (to be published).
[35] M. Kærn (unpublished).